Solar Energy Materials and Solar Cells 187 (2018) 189–193

Contents lists available at ScienceDirect

Solar Energy Materials and Solar Cells

journal homepage: www.elsevier.com/locate/solmat

Graphene oxide films for field effect surface passivation of silicon for solar cells

M. Vaqueiro-Contreras[a,*], C. Bartlam[b], R.S. Bonilla[c], V.P. Markevich[a], M.P. Halsall[a], A. Vijayaraghavan[b], A.R. Peaker[a]

[a] School of Electrical and Electronic Engineering, University of Manchester, Manchester M13 9PL, UK
[b] School of Materials, University of Manchester, Manchester M13 9PL, UK
[c] Department of Materials, University of Oxford, Oxford OX1 3PH, UK

ARTICLE INFO

Keywords:
Surface passivation
Graphene oxide
Solar cells
Dielectric charge

ABSTRACT

In recent years it has been shown that graphene oxide (GO) can be used to passivate silicon surfaces resulting in increased photocurrents in metal-insulator-semiconductor (MIS) tunneling diodes, and in improved efficiencies in Schottky-barrier solar cells with either metal or graphene barriers, however, the source of this passivation is still unclear. The suggested mechanisms responsible for the enhanced device performance include the dangling bond saturation at the surface by the diverse functional groups decorating the GO sheets which reduce the recombination sites, or field effect passivation produced by intrinsic negative surface charge of GO. In this work through a series of measurements of minority carrier lifetime with the microwave photo-conductance decay (μPCD) technique, infrared absorption spectra, and surface potential with Kelvin probe force microscopy (KPFM) we show that there is no evidence of significant chemical passivation coming from the GO films but rather negative field effect passivation. We also discuss the stability of GO's passivation and the flexibility of this material for its application as temporary passivation layer for bulk lifetime measurements, or as a potential cheap alternative to current passivation materials used in solar cell fabrication.

1. Introduction

It is well known that one of the most effective approaches to improve the efficiency of silicon-based solar cells, whilst maintaining low cost, is to increase the lifetime of photo-generated carriers by reducing recombination at the surface and in the bulk of low cost materials [1]. Therefore the study of new materials which may suppress surface recombination in such materials is important both because they may promote a minority carrier lifetime improvement in commercial solar cells but also, in the laboratory, they may allow more accurate measurements of silicon's bulk lifetime. For these reasons such new materials remain a topic of widespread interest [2–4].

Generally, for surface passivation materials we need to consider three material property aspects: the characteristics of the material to be passivated (doping type and resistivity); the physical properties of the passivating materials (optical, chemical and electrical), to determine the type of passivation that the material will provide including bond saturation, the field effect control of carriers, refractive index, and stability; and processing requirements like surface cleaning and synthesis methods. With this in mind, in this work we have studied the passivation capabilities of graphene oxide which we know fulfils some key requirements for surface passivation including: high transmittance [5], fixed surface negative charge [6,7] and high refractive index [8,9]. This is all combined with the fact that GO is water dispersible making its deposition and removal extremely simple. Most common GO deposition techniques include: dip coating, spin coating, and spray coating, techniques which can be easily incorporated to a production line. In addition, it has been recently shown that for a GO derivative dispersion with an optimal dilution, it is possible to obtain uniform coverage even on textured silicon surfaces for solar cells [10].

While passivation effects in structures incorporating GO interlayers, such as MOS and graphene/GO/Si devices, have already been reported in literature [11–16], these do not include the study of graphene oxide as a passivation material for solar cells in a scalable to manufacture system. Furthermore, to our knowledge there is no definitive answer as to what is causing the passivation on the surface from the available literature. Thus in this work we aim to answer such a question by providing strong evidence of the influence of the negative surface charge of GO in the passivation of silicon. Additionally, we demonstrate the passivation effect of GO in different silicon materials and the inclusion of GO's passivation capabilities compared to that of the industry standard material, silicon nitride (SiN_x) used for solar cell passivation

* Corresponding author.

https://doi.org/10.1016/j.solmat.2018.08.002
Received 20 February 2018; Received in revised form 29 June 2018; Accepted 2 August 2018
Available online 10 August 2018

[17] and the widespread temporary passivation attained from Iodine-Ethanol (I-E) solution immersion for bulk lifetime measurements [3].

2. Materials and methods

In this work a range of float zone (FZ) and Czochralski (Cz) grown, boron-doped silicon wafers with ‹100› crystal orientation, double (DSP) and single (SSP) side polished, with resistivities between 1 and 1000 Ω·cm, and thicknesses from 200 to 625 μm have been used to study the passivation effect of GO. Most of the measurements were carried out in cut samples of $2 \times 2\,cm^2$ which were subjected to the standard cleaning "RCA 1" procedure as described in Ref. [18]. However, the usually applied subsequent HF dip of the samples was not performed since it was found that such step resulted in a diminished passivation of the silicon surface due to the lack of hydrophilicity on the surface provided by either the native oxide or the oxide left by the H_2O_2. It must be noted as well that the samples were cleaned and left in the desiccator for at least 3 days before the GO deposition, and their lifetime measured before and after the deposition to avoid the inclusion of the RCA 1 passivation effect into consideration, it was determined that this process takes place within that period before stabilisation.

GO was prepared by a modified Hummers method [19] whereby natural flake graphite (30 mesh, 96%C) was oxidised and exfoliated. Sulphuric acid (H_2SO_4, 98%), hydrogen peroxide (H_2O_2, 30%), ammonium hydroxide (NH_4OH, 35%) (Sigma Aldrich); sodium nitrate and potassium permanganate ($KMnO_4$, Alfa Aesar) were all used as supplied and without any further purification. The oxidised graphite was repeatedly washed and exfoliated using a 3% wt. H_2SO_4/ 0.5% wt. H_2O_2 mixture and then washed further with deionised water until a pH of 7 was reached for the supernatant to ensure the removal of the H_2SO_4. The GO pellet had a pH of 3.6. To adjust the pH of GO, 100 μl of ammonium hydroxide was added to under stir to give a pH of 9.9 ± 0.01 measured with a Mettler Toledo F20 pH meter.

For the silicon nitride deposition we used the Plasma-Enhanced Chemical Vapour Deposition (PECVD) technique for 2 min, to achieve a film thickness of 90 nm ± 3 nm according to spectroscopic ellipsometry. This was done on a PlasmaPro 100 PECVD system from Oxford Instruments with: 20:20 sccm SiH4: NH3 gas flow, 300 mTorr chamber pressure, 400 °C table temperature, 13.56 MHz plasma generated frequency and 50 W of power as deposition parameters.

Kelvin Probe force microscopy on the PeakForce tapping frequency-modulated mode (FM-KPFM) using SCM-PIT-V2 tips was used to map the surface potential of single GO flakes on a Bruker Dimension FastScan. Samples for this measurements were prepared by spin coating 0.5 mg/ml of GO for 60 s at a speed of 1000 rpm and left to dry on a desiccator overnight. Infrared absorption spectroscopy on 200 nm ± 20 nm thick GO coated silicon samples was carried out with a Hyperion 3000 FT-IR microscope with a resolution of $4\,cm^{-1}$ in transmission mode.

A Semilab WT-2000 PVN was used for minority carrier lifetime mapping by the microwave photoconductivity decay (μPCD) technique, with a 905 nm LASER excitation and a microwave source operating at ~10 GHz. Hence the presented effective lifetime maps show the averaged lifetime down to a few tens of microns into the sample. The level of passivation achieved by GO layers was tested in several samples by the measurement of their effective lifetime (τ_{eff}) by μPCD mapping, with the assumption that both sides of each sample were equally passivated. Next, what is considered the upper limit of the surface recombination velocity (S_{UL}) was calculated by assuming the bulks lifetime (τ_{bulk}) to be infinite, thus giving $S_{UL} = W/2(\tau_{eff})$, with W representing the sample thickness.

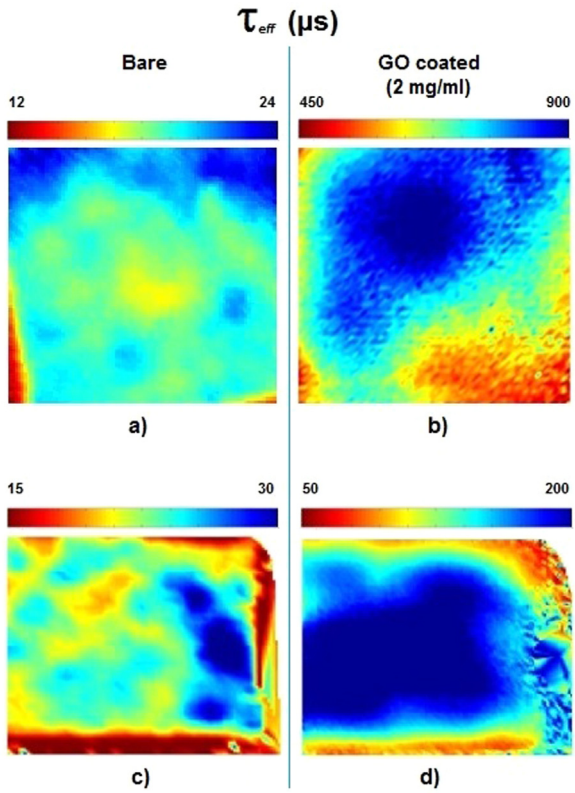

Fig. 1. Effective lifetime maps of a DSP FZ p-type (> 1000 Ω·cm) silicon sample (a) bare and (b) GO coated, and a SSP Cz p-type (2.8 Ω·cm) silicon sample (c) bare and GO coated.

3. Results and discussion

3.1. GO effect on minority carrier lifetime

We have carried out transient photoconductance mapping to compare the level of surface passivation achieved by GO in various sets of samples, here we present the comparison of GO's passivation on an electronic grade FZ material to that of a solar grade Cz material. Fig. 1 show the lifetime maps of the FZ and the Cz boron doped samples before (**a**, **c**), and after (**b**, **d**) GO passivation, respectively. For the FZ sample it can be observed that the τ_{eff} approaches 1 ms in some areas. Nevertheless, considering the maximum effective lifetime in the sample to be τ_{max} = 900 μs and W = 500 μm we obtain a $S_{UL} \approx 27\,cm\,s^{-1}$, whereas from the τ_{max} = 820 μs and W = 200 μm of the Cz sample the calculation results in a $S_{UL} \approx 30\,cm\,s^{-1}$. These values are comparable to the surface recombination velocities of some existent surface passivation materials [3,4]. Moreover, we have compared the surface passivation of GO to that of PECVD deposited SiN_x and I-E solution immersion. The passivation was carried out on samples cut from a solar grade SSP Cz p-type wafer (25 ± 7.5 Ω·cm), the lifetime comparison is presented in Fig. 2. The calculated upper limit surface recombination velocities from each sample are: $363\,cm\,s^{-1}$, $322\,cm\,s^{-1}$ and $202\,cm\,s^{-1}$ for GO (Fig. 2a), I-E (Fig. 2b) and SiN_x (Fig. 2c), respectively. These results indicate that in some silicon materials it is possible to attain very similar levels of surface passivation with GO coatings to those obtained by the widely used SiN_x and I-E techniques.

With respect to the surface passivation stability we have found that the GO passivation effect can last for several days, however there appears to be some unpredictable behaviour in GO's passivation after storage. We have observed there is an increase in averaged lifetime after a few days of air ambient storage of the samples, which we suggest to be attributed to the interlayer water molecule release which

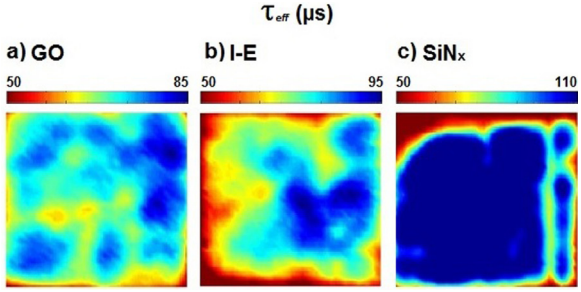

Fig. 2. Effective lifetime maps of samples cut from a B-doped Cz wafer of thickness 625 ± 25 μm, passivated with (a) 4 mg/ml GO, (b) I-E solution, and (c) PECVD SiN_x.

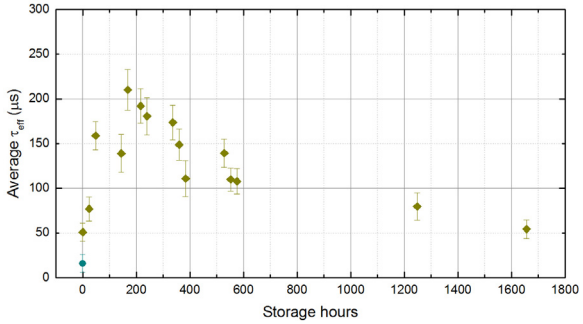

Fig. 3. Averaged effective lifetime values of samples cut from a B-doped Cz wafer of thickness 200 ± 5 μm. Initial non-passivated value is identified with the circular marker, whereas the diamond marker represents the passivated averaged values with 2 mg/ml GO after air ambient storage.

decreases the spacing between GO sheets and increases the negative charge on the surface. Thus, after reaching an average τ_{eff} maxima, the lifetime begins to decrease slowly as shown in Fig. 3, where effective lifetime degradation is shown for a B-doped (2.8 Ω·cm), SSP, Cz grown silicon sample coated with 2 mg/ml GO after air storage during 70 days. It must be noted that Fig. 3 shows the averaged effective lifetimes of $3 \times 3\,cm^2$ samples with some deviations due to GO aggregation sites, thus making it difficult to appreciate the amount of stability obtained within the first two weeks of deposition. The data point with a circular marker in Fig. 3 represents the averaged lifetime of the bare sample which in comparison to the data taken after 1600 h shows that even after the 70 day lifetime degradation there is still some passivation present from the GO coating. We believe that it may be possible to improve the stability with the application of an encapsulation or capping method. This approach would avoid the gradual reduction of dried GO at ambient conditions in the presence of humidity and high pH which is likely to be the cause of the passivation degradation.

3.2. Passivation mechanism

We have demonstrated the capability of GO to passivate silicon surfaces by τ_{eff} mapping of silicon samples. This is in line with the observations of higher efficiencies from some authors in literature [11–16], however the mechanism responsible of the passivation is still under debate. On the one hand Yang et al. [14] has suggested the passivation to be due to surface dangling bond saturation provided by the hydroxyl and carbonyl groups which decorate the graphene-like sheet of GO, whereas Hsu et al. [12] and Jiao et al. [13] attribute the passivation to the negative surface charge of GO. Henceforth we provide some evidence to support the latter as the source of the passivation.

It has been largely acknowledged in the literature that the abundant oxygen containing functional groups of GO such as: hydroxyls (C-OH), carboxyls (COOH), and epoxides (C-O-C) are the source of a strong negative surface charge in the GO sheets [7,20,21]. Even though there still exist some dispute on the distribution of these functional groups and their impact on GO's properties, the negative charge attributed to them has been accepted by the 2D material community. GO's negative charge has been observed to be significantly dependent on the pH of GO's colloidal dispersion, and has been measured mostly by the zeta potential technique [16,22–24] and more recently by Kelvin-probe microscopy [25]. In this work we have thus studied the impact of pH on the surface passivation ability of GO in a range of samples, primarily observing the effect of low (3.6 ± 0.01) and high (10 ± 0.01) pH GO solutions in the passivation, this because there were no observable trends from intermediate values as could be expected from the small zeta potential increase in mid values reported in various references [16,22–24].

Firstly, to observe the effect of pH on the surface potential of the GO single flakes (see Fig. 4**a** and **b** for topography illustration) we used the PeakForce-KPFM technique on both materials. Images of the measurements are shown in Fig. 4**c** and **d** for the low and high pH dispersions, respectively. A cross-section profile of the measured surface potential is also shown in Fig. 4 for both pH's. From these measurements the contact potential difference (V_{CPD}) between the tip and the sample presents a threefold increase in negative potential going from V_{CPD} = 24 ± 7 mV for the low pH GO flake to V_{CPD} = 62 ± 4 mV for the high pH GO flake. These results indicate that there is indeed an increase

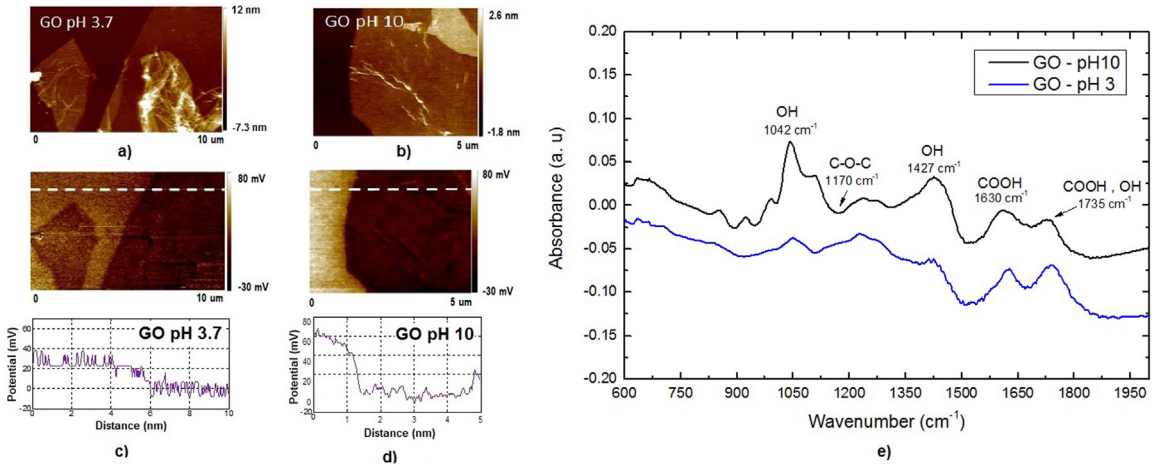

Fig. 4. AFM images of sheets from a low (a) and high (b) pH GO dispersion. PeakForce-KPFM maps from the same GO sheets with low (c) and high (d) pH. (e) Transmission IR absorption spectra from silicon samples coated with low and high pH 3 mg/ml GO.

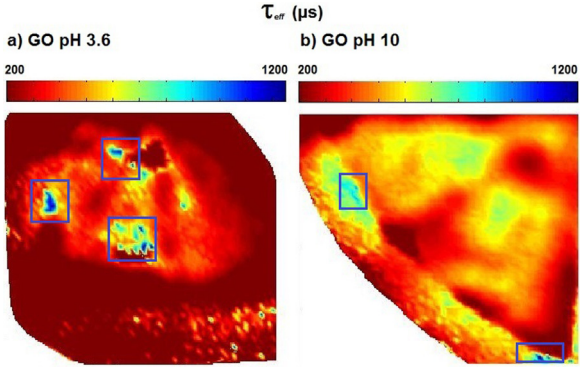

Fig. 5. Effective lifetime maps of samples cut from a B-doped FZ wafer of thickness 300 ± 5 μm, passivated with 2 mg/ml GO with (a) pH 3.6 (as prepared) and (b) pH 10. The blue boxes highlight the highest lifetime areas.

in negative charges on each GO flake from the basic solution. Moreover an increase in potential with number of GO layers was observed, confirming the results reported by Salomao et al. in [26]. We have carried out FTIR measurements on silicon samples coated with thick layers of the same low and high pH GO dispersions to correlate with functional group content, results are shown in Fig. 4**e**. The IR spectra at distinct points of the sample show a rather significant increase in the vibrational frequencies 1042 cm^{-1} and 1427 cm^{-1} typically assigned to hydroxyl groups, some increase in the range 1600 − 1750 cm^{-1}, frequencies commonly assigned to carboxyl and hydroxyl groups and a slight decrease in the band 1170 cm^{-1} assigned to the epoxides [27]. This evidence adds to the argument of having the oxygen-containing groups as the source of negative charge in GO. We then performed photoconductance decay measurements to compare the passivation level attained with each material. In Fig. 5**a** and **b** we show the compared τ_{eff} maps of samples taken from a high resitivity p-type FZ wafer passivated with 2 mg/ml GO solutions with low and high pH, respectively. In these samples the averaged τ_{eff} increased from 236 μs in the low pH sample to 389 μs in the high pH sample, suggesting that the added negative charge from the hydroxyl groups improves the passivation. In terms of S_{UL} however, we calculated a value of 17.4 cm s^{-1} for the low pH sample and 19.5 cm s^{-1} for the high pH sample, considering the τ_{max} measured of 1430 μs and 1282 μs respectively for each sample, these high lifetime areas have been highlighted in Fig. 5. On these areas, an increase of a few tens of nm in GO thickness was measured, indicating that these effect may be the result of a higher aggregation of GO sheets in the low pH solution [22,24] which in turn increases the net negative charge in the area and consequently the field effect passivation. This is in agreement with the negative field effect passivation obtained with GO coating. It must be also noted that, as mentioned in the methods section, the passivation of GO was significantly decreased by the oxide removal from the samples. This fact suggests that there is no dangling bond saturation involved in the passivation mechanism of GO, since a SiO_2 thin interlayer (less than 10 nm) has been found to be required for an improved passivation. Such observations contradict the possibility of physical bonding between GO's functional groups and silicon atoms at the surface as suggested by Yang et al. in [14].

4. Conclusions

In this work we have reported the effectiveness of graphene oxide as a surface passivation coating for silicon solar cells. Surface recombination velocities as low as 14.4 cm s^{-1} have been obtained. Studies on the passivation mechanism attained by GO and its stability are discussed. We found the passivation to be likely explained by the negative fixed charge coming from the oxygen-containing groups, hydroxyl groups in particular, surrounding the GO's flakes and discard previous suggestions of predominant chemical passivation. The simplicity of GO's deposition and removal without surface damage make this process a good alternative for temporary surface passivation for bulk lifetime measurements. Furthermore, with the use of an appropriate encapsulation method or capping layer deposition, results in here presented demonstrate that GO can be a potential cheap and low risk alternative to currently used surface passivation materials for silicon-based solar cells.

Acknowledgments

We would like to thank Engineering and Physical Sciences Research Council, (EPSRC), United Kingdom for funding under contract under the SuperSilicon PV contract (EP/M024911/1). Financial support was also given by Consejo Nacional de Ciencia y Tecnologia, Mexico CONACyT-Mexico. R.S. Bonilla is the recipient of an EPSRC (UK) Postdoctoral Research Fellowship, EP/M022196/1.

References

[1] M.A. Green, S.P. Bremner, Energy conversion approaches and materials for high efficiency photovoltaics, Nat. Mater. 16 (2017) 23–34.
[2] R.S. Bonilla, C. Reichel, M. Hermle, P.R. Wilshaw, Extremely low surface recombination in 1 $Ω$ cm n-type monocrystalline silicon, Phys. Status Solidi - Rapid Res. Lett. 11 (2017) 1600307.
[3] N.E. Grant, J.D. Murphy, Temporary surface passivation for characterisation of bulk defects in silicon: a review, Phys. Status Solidi - Rapid Res. Lett. 11 (2017).
[4] R.S. Bonilla, B. Hoex, P. Hamer, P.R. Wilshaw, Dielectric surface passivation for silicon solar cells: a review, Phys. Status Solidi 214 (2017) 1700293.
[5] H.A. Becerril, J. Mao, Z. Liu, R.M. Stoltenberg, Z. Bao, Y. Chen, Evaluation of solution-processed reduced graphene oxide films as transparent conductors, ACS Nano. 2 (2008) 463–470.
[6] A. Lerf, H. He, M. Forster, J. Klinowski, Structure of graphite oxide revisited, J. Phys. Chem. B. 102 (1998) 4477–4482.
[7] D. Chen, H. Feng, J. Li, Graphene oxide: preparation, functionalization, and electrochemical applications, Chem. Rev. 112 (2012) 6027–6053.
[8] I. Jung, M. Vaupel, M. Pelton, R. Piner, D.A. Dikin, S. Stankovich, J. An, R.S. Ruoff, Characterization of thermally reduced graphene oxide by imaging ellipsometry, J. Phys. Chem. C. 112 (2008) 8499–8506.
[9] L.-C. Chen, C.-T. Yu, Y.-C. Peng, J.-J. Hung, H.-M. Chang, S.-D. Tzeng, C.-M. Wang, C.-C. Lin, C.-H. Lin, Antireflection with graphene oxide, Opt. Mater. Express 6 (2016) 8.
[10] A. Nandi, S. Majumdar, S.K. Datta, H. Saha, S.M. Hossain, Optical and electrical effects of thin reduced graphene oxide layers on textured wafer-based c-Si solar cells for enhanced performance, J. Mater. Chem. C 5 (2016) 1920–1934.
[11] C.H. Lin, W.T. Yeh, M.H. Chen, Metal-insulator-semiconductor photodetectors with different coverage ratios of graphene oxide, IEEE J. Sel. Top. Quantum Electron. 20 (2014).
[12] W.-T. Hsu, Z.-S. Tsai, L.-C. Chen, G.-Y. Chen, C.-C. Lin, M.-H. Chen, J.-M. Song, C.-H. Lin, Passivation ability of graphene oxide demonstrated by two-different-metal solar cells, Nanoscale Res. Lett. 9 (2014) 1–5.
[13] K. Jiao, X. Wang, Y. Wang, Y. Chen, Graphene oxide as an effective interfacial layer for enhanced graphene/silicon solar cell performance, J. Mater. Chem. C 2 (2014) 7715.
[14] L. Yang, X. Yu, M. Xu, H. Chen, D. Yang, Interface engineering for efficient and stable chemical-doping-free graphene-on-silicon solar cells by introducing a graphene oxide interlayer, J. Mater. Chem. A 2 (2014) 16877–16883, https://doi.org/10.1039/C4TA02216E.
[15] L. Lancellotti, L. Sansone, E. Bobeico, E. Lago, M. Della Noce, P. Delli Veneri, A. Borriello, M. Casalino, G. Coppola, M, I.M. Giordano, Graphene oxide as an interfacial layer in silicon based schottky barrier solar cells, IET Conf. Publ. 2015 (2015) 1–4.
[16] V. Georgakilas, J.N. Tiwari, K.C. Kemp, J.A. Perman, A.B. Bourlinos, K.S. Kim, R. Zboril, Noncovalent Funct. Graph. Graph. Oxide Energy Mater., Biosensing, Catal., Biomed. Appl. (2016).
[17] A. Aberle, Overview on SiN surface passivation of crystalline silicon solar cells, Sol. Energy Mater. Sol. Cells 65 (2001) 239–248.
[18] W. Kern, J.E. Soc, The evolution of silicon wafer cleaning technology, J. Electrochem. Soc. 137 (1990) 1887–1892.
[19] J.P. Rourke, P.A. Pandey, J.J. Moore, M. Bates, I.A. Kinloch, R.J. Young, N.R. Wilson, The real graphene oxide revealed: stripping the oxidative debris from the graphene-like sheets, Angew. Chem. - Int. Ed. 50 (2011) 3173–3177.
[20] M. Li, C. Liu, Y. Xie, H. Cao, H. Zhao, Y. Zhang, The evolution of surface charge on graphene oxide during the reduction and its application in electroanalysis, Carbon N. Y 66 (2014) 302–311.
[21] M.M. Gudarzi, Colloidal stability of graphene oxide: aggregation in Two Dimensions, Langmuir 32 (2016) 5058–5068.
[22] C.J. Shih, S. Lin, R. Sharma, M.S. Strano, D. Blankschtein, Understanding the pH-dependent behavior of graphene oxide aqueous solutions: a comparative experimental and molecular dynamics simulation study, Langmuir 28 (2012) 235–241.

[23] D. Li, M.B. Mueller, S. Gilje, R.B. Kaner, G.G. Wallace, Processable aqueous dispersions of graphene nanosheets, Nat. Nanotechnol. 3 (2008) 101–105.
[24] S. a. Hasan, J.L. Rigueur, R.R. Harl, A.J. Krejci, I. Gonzalo-Juan, B.R. Rogers, J.H. Dickerson, SI-Transferable graphene oxide films with tunable microstructures, ACS Nano. 4 (2010) 7367–7372.
[25] M. Jaafar, Step like surface potential on few layered graphene oxide Step like surface potential on few layered graphene oxide, Appl Phys Lett. 101, 2012, 263109.
[26] F.C. Salomão, E.M. Lanzoni, C.A. Costa, C. Deneke, E.B. Barros, Determination of high-frequency dielectric constant and surface potential of graphene oxide and influence of humidity by kelvin probe force microscopy, Langmuir 31 (2015) 11339–11343.
[27] M. Acik, G. Lee, C. Mattevi, A. Pirkle, R.M. Wallace, M. Chhowalla, K. Cho, Y. Chabal, The role of oxygen during thermal reduction of graphene oxide studied by infrared absorption spectroscopy, J. Phys. Chem. C. 115 (2011) 19761–19781.